BIOCHEMISTRY
including biophysical chemistry & molecular biology

Article

pubs.acs.org/biochemistry

Partial Unfolding of a Monoclonal Antibody: Role of a Single Domain in Driving Protein Aggregation

Shyam B. Mehta,[†] Jared S. Bee,[‡] Theodore W. Randolph,[§] and John F. Carpenter*,[†]

[†]Department of Pharmaceutical Sciences, University of Colorado Anschutz Medical Campus, Aurora, Colorado 80045, United States
[‡]Formulation Sciences Department, MedImmune, Gaithersburg, Maryland 20878, United States
[§]Department of Chemical and Biological Engineering, University of Colorado, Boulder, Colorado 80309, United States

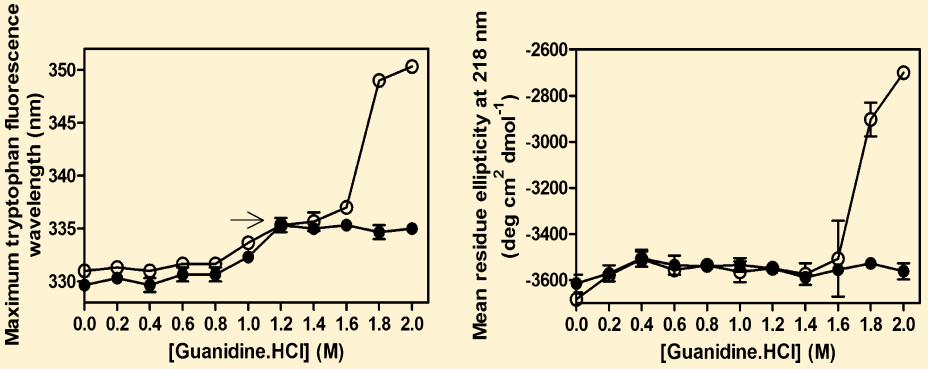

ABSTRACT: We have examined the effect of incubating a monoclonal antibody (mAb) in low (0−2.0 M) concentrations of guanidine hydrochloride (GdnHCl) on the protein's conformation and aggregation during isothermal incubation. In GdnHCl solutions at concentrations from 1.2 to 1.6 M, the mAb was partially unfolded. As demonstrated by fluorescence and circular dichroism spectroscopy, the partially unfolded state of the antibody had perturbed tertiary structure but retained native secondary structure. Furthermore, partial unfolding of the antibody was documented by analytical ultracentrifugation, dynamic light scattering, and limited proteolysis. Subsequent aggregation of the antibody was characterized using size-exclusion chromatography, analytical ultracentrifugation, and dynamic light scattering. Over the entire concentration range (0−2.0 M) of GdnHCl, protein−protein interactions were attractive, as quantified by negative osmotic second virial coefficients measured with static light scattering. However, during isothermal incubation at 37 °C, the aggregation of the antibody was detected only in solutions that induced partial unfolding. Differential scanning calorimetry studies showed that the antibody's C_H2 domains were unfolded in antibody molecules that had been incubated in 1.2 M and higher concentrations of GdnHCl. These results suggest that unfolding of the C_H2 domains leads to aggregation.

Protein aggregation is implicated in numerous diseases such as Alzheimer's disease, Parkinson's disease, and systemic amyloidosis.[1−5] Control of protein aggregation is also important for the development of therapeutic protein products.[6,7] During development of protein drugs, aggregation may be encountered during all phases of processing such as purification, shipping, storage, and even during administration to patients.[8−12] There is great concern about aggregates in therapeutic products, because administration of protein aggregates into patients may cause adverse reactions such as unwanted immune response and anaphylactic shock.[11,12]

Thus, it is critical that aggregate levels in therapeutic protein products are controlled and minimized. In turn, it is important to understand the mechanisms for protein aggregation and to develop strategies to reduce this form of degradation. Key in these efforts is identifying the species in a population of protein molecules that are prone to react to form aggregates.

Early studies led to the proposal that fully unfolded protein molecules react to form aggregates.[13−15] However, in several more recent studies, it was observed that aggregates can form from partially unfolded protein molecules[6,16−24] that have perturbed tertiary structure but native-like secondary structure.[18] In addition, some studies have documented that these partially unfolded species are constituents of the native-state ensemble of substates.[25]

Therefore, even under conditions that thermodynamically favor the native state, protein aggregates can form. Furthermore, the aggregation-prone protein molecules are typically at extremely low levels[26,27] so that even modest increases in the absolute concentrations of these reactive species can substantially increase aggregation rates. For example, earlier studies on therapeutic proteins have shown how changes in solution pH[16] or addition of antimicrobial preservative such as benzyl alcohol[28−32] can stimulate large

Received: February 19, 2014
Revised: April 11, 2014
Published: May 7, 2014

   dx.doi.org/10.1021/bi5002163 | *Biochemistry* 2014, 53, 3367−3377

increases in aggregation rate by causing relatively modest shifts in the protein population toward partially unfolded species.

Most studies showing that partial unfolding leads to aggregation have focused on relatively small, single-domain proteins like apomyoglobin,[33] RNase A,[34] and cytochrome c.[28] Aggregation of small therapeutic proteins like G-CSF[32,35] and rhIL-1ra[30,31,36] has also been shown to occur via partial unfolding.

Multidomain proteins may also aggregate as a result of unfolding of one or more domains. For example, Souillac et al. have shown that for an IgG1 molecule the observed aggregates were due to association of C_H3 domains.[37] Several other studies on antibody molecules have shown that the C_H2 domain is involved in the process of aggregation.[38,39] Other works carried out on multidomain proteins, which are not antibody molecules, have shown that the least stable domain of the molecule is involved in the aggregation process.[40−42] Oligomerization of multidomain proteins has also been shown to occur via domain swapping,[43] in which one protein molecule exchanges a domain with an identical molecule, forming an oligomer.

Physical instability of monoclonal antibodies (mAbs) is of great concern in the field of pharmaceutical biotechnology. Recently, it has been shown that exposure to low pH or high ionic strength can stimulate aggregation of mAbs by favoring formation of partially unfolded protein molecules.[44−46] Studies of antibody aggregation under such pharmaceutically relevant stresses also have tried to identify specific domains in the protein molecule that unfold and are responsible for aggregation. For instance, Kim et al. showed that F_{ab} unfolding caused by low pH or high salt concentration led to aggregation of an IgG1 molecule.[47] On the other hand, Majumdar et al. showed that aggregation caused by high concentrations of salts was mediated by C_H2 instability.[38]

Addition of chaotropes has long been used to perturb protein structure in order to study populations of partially and fully unfolded molecules.[48−50] Furthermore, some studies have shown that partially unfolded species populated in low concentrations of denaturant readily aggregate.[51,52,53] In contrast, it is commonly observed that proteins do not aggregate in solutions that contain denaturant concentrations that result in complete unfolding. For example, proteins purified from bacterial inclusion bodies are routinely unfolded and solubilized in concentrated GdnHCl[54,55] and do not aggregate until refolding is initiated by reducing the denaturant concentration.[56,57]

Protein aggregation also has been shown to be controlled by protein−protein interaction energetics, which is a function of protein conformation and solvents.[6,40,58] Static light scattering is a powerful tool to study protein−protein interactions in solution. Static light scattering can be used to investigate the osmotic second virial coefficient (B_{22}), which is a measure of strength of net protein−protein interactions. A positive value of B_{22} indicates repulsive forces between protein molecules, whereas a negative value indicates attractive interactions.[59,60] Protein−protein interactions can be affected by solution conditions such as pH and ionic strength, sometimes independent of effects on conformational stability.[6]

In our study, we used various concentrations of GdnHCl to alter protein conformation in a model mAb such that the protein structure ranged from native to partially to fully unfolded. We found that at intermediate concentrations of GdnHCl only certain domains of the protein were perturbed, whereas the overall secondary structure was not altered. Our hypothesis was that partially unfolded species of a mAb (formed at low concentrations of GdnHCl) would aggregate, whereas native, folded mAb or fully unfolded mAb molecules (found at high denaturant concentrations) would not. Furthermore, we measured protein−protein interaction energetics as a function of GdnHCl concentration to probe the importance of colloidal stability in denaturant-induced protein aggregation.

To test our hypothesis, we determined the equilibrium unfolding curve for the mAb. Furthermore, we used circular dichroism (CD), fluorescence spectroscopy, limited proteolysis, analytical ultracentrifugation, and differential scanning calorimetry to characterize the protein's structure and to identify the domains perturbed by GdnHCl. In addition, we used light scattering to determine protein−protein interaction energetics of the mAb in various concentrations of GdnHCl. Finally, protein aggregation was quantified with size-exclusion chromatography, dynamic light scattering, and analytical ultracentrifugation.

EXPERIMENTAL PROCEDURES

Materials. Purified mAb was provided by MedImmune (Gaithersburg, MD) in a lyophilized form. The lyophilized material was reconstituted with 2.2 mL of water for injection (WFI) to obtain 50 mg mL^{-1} protein in 10 mM histidine, 6% trehalose, 2% arginine, and 0.025% PS80 at pH 6.0. USP grade reagents such as 2-(*N*-morpholino)ethanesulfonic acid (MES) and guanidine hydrochloride (GdnHCl) were purchased from Fisher Scientific (Fair Lawn, NJ). Unless otherwise indicated, deionized Milli-Q water was used to prepare all solutions. Lyophilization vials (3 mL) and caps were purchased from West Pharmaceutical (Lionville, PA). Cuvettes used for CD and fluorescence spectroscopy were purchased from Starna Cells (Atascadero, CA).

Protein Sample Preparation. The reconstituted protein concentration was determined using an Agilent 8540 spectrophotometer (Santa Clara, CA) with an extinction coefficient of 1.45 mL mg^{-1} cm^{-1} at 280 nm. The concentration of stock protein solution was estimated to be 50 mg mL^{-1}. For experiments, the stock protein solution was diluted into different concentrations of GdnHCl to give the desired final denaturant concentration and a final protein concentration of 1 mg mL^{-1}. A stock solution of 7.0 M GdnHCl in 10 mM MES (pH 6.0) was used. Stock GdnHCl concentration was determined using refractive index measurements.[61]

Antibody Unfolding Curve. Far-UV CD spectra were collected for protein equilibrated in different concentrations of GdnHCl using a Chirascan-plus spectrometer (Applied Photophysics, UK) and a 1 mm path-length cuvette. Protein at 1.0 mg mL^{-1} was allowed to equilibrate in several concentrations of GdnHCl at 37 °C for 1 day. The CD signal at 218 nm was monitored as a function of GdnHCl concentration to obtain the unfolding curve. Triplicate samples were analyzed for each concentration of GdnHCl, and one scan per sample was collected.

Fluorescence and Circular Dichroism Spectroscopy. The mAb, at a concentration of 1 mg mL^{-1}, was incubated in 0−2.0 M GdnHCl solutions at 0.2 M increments. Triplicate samples were incubated at 37 °C and were analyzed using fluorescence and CD spectroscopy on days 0, 1, 6, and 11 of incubation. For each sample, one spectrum was recorded.

Intrinsic tryptophan fluorescence spectra were acquired using Photon Technology International (PTI) spectrofluorometer (Lawrenceville, NJ). Tryptophan (Trp) excitation was carried out using a 295 nm wavelength, and emission spectra were collected from 300 to 400 nm with a 1 nm s^{-1} data collection rate and 1 s integration time. The slit widths for Trp excitation and emission were 4 and 1 nm, respectively. The maximum tryptophan fluorescence peak position was obtained by calculating the first derivative of the emission spectrum. We also calculated the tryptophan fluorescence center of mass by integrating the emission spectrum.[62] Far-UV CD spectra were collected for incubated protein samples using a Chirascan-plus spectrometer (Applied Photophysics, UK) in 1 mm path-length cuvettes. For each time point of the incubation, the CD signal at 218 nm was plotted as a function of GdnHCl concentration.

Static Light Scattering. We used a Brookhaven light scattering system (Brookhaven Instruments Corporation, Holtsville, NY) to obtain static light scattering (SLS) measurements. Protein samples were prepared at concentrations ranging from 0.5 to 5.0 mg mL^{-1} in various concentrations of GdnHCl, and the scattering intensity was measured at 90°. Triplicate samples were prepared for each condition, and scattering intensity was acquired for each sample replicate. All buffers were filtered using 0.02 μm Anotop 25 syringe filters (Whatman International Ltd.). The relationship used to determine B_{22} is derived from the virial expansion of the ideal osmotic pressure equation[63]

$$\frac{Kc}{R_{90}} = \frac{1}{M} + 2B_{22}c \tag{1}$$

where c is the protein concentration (g mL^{-1}), K is the optical density constant (mL mol g^{-2} cm^{-1}), M is the protein molecular weight (g mol^{-1}), R_{90} is the excess Rayleigh ratio at 90° (cm), and B_{22} is the second osmotic virial coefficient (mL mol g^{-2}). B_{22} values determined from eq 1 were scaled by the theoretical value of the hard sphere (HS) second virial coefficient to obtain $b_2^* = (B_{22}/B_{22}^{HS}) - 1$, where $B_{22}^{HS} = (2/3)\pi d^3$ and d is the effective HS diameter for a monomer.[44] As an estimate of the HS diameter, the hydrodynamic diameter (11.4 nm) was determined using dynamic light scattering (DLS) as described below.

Size-Exclusion Chromatography. On days 0, 1, 6 and 11, SEC analysis of triplicate mAb samples that had been incubated at 37 °C was performed to determine monomer and soluble aggregate levels. A Tosoh TSKgel G3000SWXL was used, and protein in the eluate was quantified using absorbance at 280 nm. Prior to loading the sample in a given concentration of GdnHCl, the column was equilibrated with one column volume of that particular concentration of GdnHCl in 0.1 M Na_2SO_4, 0.1 M Na_2HPO_4, pH 6.8, which was also used as the mobile phase at a flow rate of 1 mL min^{-1}. Percent recoveries of soluble protein and percent soluble aggregates were calculated by normalizing against total peak area of chromatograms for day 0 samples. Only monomeric mAb was detected by SEC in day 0 samples.

Dynamic Light Scattering To Determine mAb Hydrodynamic Diameter. On days 0, 1, 6, and 11, DLS analysis of triplicate mAb samples that had been incubated at 37 °C was performed to determine the hydrodynamic diameter of the mAb using a Zetasizer Nano ZS (Malvern, UK). Hydrodynamic diameters were calculated from measured diffusion coefficients and values of solution viscosity using the Stokes−Einstein equation[64]

$$D = \frac{k_B T}{6\pi\eta r} \tag{2}$$

where k_B is Boltzmann's constant, T is absolute temperature, η is viscosity of solvent containing GdnHCl, and r is the hydrodynamic radius. Cumulant analysis was performed for each sample. Viscosities as a function of GdnHCl were estimated using the public domain software program SEDNTERP.[65]

Analytical Ultracentrifugation . On days 0, 1, 6, and 11, AUC analysis of mAb samples that had been incubated at 37 °C was performed using the sedimentation velocity obtained with a Beckman XL-A analytical ultracentrifuge equipped with absorbance optics. Samples prepared in each concentration of GdnHCl were sedimented at 25 °C at rotor speed of 40 000 rpm, and data were collected at 294 nm. The raw data collected from sedimentation velocity experiments were analyzed using software program SEDFIT.[65] The meniscus position was allowed to vary as a fitted parameter, and the cell bottom position was fixed at 7.2 cm.[66] The frictional ratio (f/f_0 = 1.5) and mAb partial specific volume (ν = 0.727 L kg^{-1}) suggested by Arthur et al. were used.[66] Buffer densities and viscosities for each concentrations of GdnHCl were calculated using the public domain software program SEDNTERP.[65] The sedimentation coefficient values of monomer were corrected to standard conditions of water at 20 °C using the formula[65]

$$s_{20,w} = s_{T,B}\left(\frac{\eta_{T,B}}{\eta_{20}}\right)\left(\frac{1 - \nu\rho_{20}}{1 - \nu\rho_{T,B}}\right) \tag{3}$$

where T and B denote the values at the temperature and under the buffer conditions of the experiment, respectively, and index 20,w indicates standard conditions.

Ellman's Reagent Test and Quantification of Covalent Aggregates. To ascertain if the mAb had any free cysteines that might play a role in aggregate formation, we checked for reactivity of Ellman's reagent (5,5′-dithiobis(2-nitrobenzoic acid) or DTNB) with mAb as a function of GdnHCl concentration. Briefly, 2 mM Ellman's reagent was added to 30 μM protein samples on days 0 and 1. Absorbance at 412 nm was measured using an Agilent 8540 spectrophotometer (Santa Clara, CA). The presence of covalent aggregates was quantified using a SDS-PAGE gel. For each time point, mAb samples incubated at 37 °C in 1, 1.2, 1.4, 1.6, 1.8, or 2 M GdnHCl were run on an SDS-PAGE gel. The intensity of each band corresponding to covalent aggregate was calculated using Quantity One software on a Bio-Rad Gel Doc XR+ instrument.

Proteinase K Assay and SDS-PAGE. In order to characterize partially unfolded protein species, a proteinase K assay[67−69] was conducted for mAb samples incubated in 0.6, 1.0, 1.2, 1.4, 1.6, 1.8, and 2 M GdnHCl. The supplier of the proteinase K has shown that the enzyme maintains activity in GdnHCl solutions at concentrations up to 3 M GdnHCl (5 PRIME, Gaithersburg, MD.). Proteinase K (20 ng in 5 μL) was added to 50 μL of a 1 mg mL^{-1} solution of mAb. The samples were incubated at 37 °C for 1 h. After incubation, proteins in the samples were precipitated by addition of 12 μL of trichloroacetic acid (TCA). After 10 min of incubation on ice, the samples were centrifuged at 14 100g for 5 min. Supernatant was removed from the centrifuged sample, leaving the protein pellet intact. The pellet was washed with 200 μL of ice-cold acetone, and the tubes were centrifuged at 14 100g for 5 min. Pellets were washed 2× with ice-cold acetone and dried

dx.doi.org/10.1021/bi5002163 | Biochemistry 2014, 53, 3367−3377

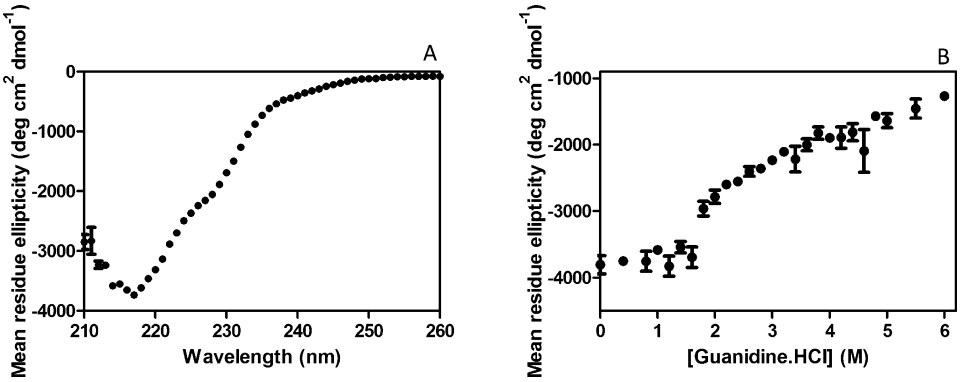

Figure 1. (A) Far-UV CD spectrum for mAb at 1 mg mL^{-1}. The CD signal at 218 nm was followed as a function of GdnHCl concentration to obtain the denaturation curve for the mAb. (B) Mean residue molar ellipticity at 218 nm as a function of GdnHCl concentration. Data points represent the mean ± SD for triplicate samples. Error bars for certain data points are smaller than their associated symbols.

at 95 °C using a heat block for 5−10 min. The tubes were removed, and 40 μL of 10% SDS and 10 μL of 4× loading dye were added to each sample pellet. The samples were boiled for 5 min at 95 °C using a heat block. The samples were centrifuged at 14 100*g* for 5 min before loading 15 μL of each sample on an SDS-PAGE gel. As a control, nondigested mAb was subjected to the TCA precipitation protocol to observe the effect of TCA on protein. The SDS-PAGE gel was stained with Coomassie blue stain and washed prior to obtaining the gel image.

Differential Scanning Calorimetry. The stability and domain unfolding of mAb in various concentrations of GdnHCl was determined using a VP-capillary differential scanning calorimeter (MicroCal, Northampton, MA). Samples were mixed and held at room temperature, and DSC analysis was performed within 30 min of sample preparation. Protein samples at 1 mg mL^{-1} were analyzed over a temperature range of 10−90 °C at a scan rate of 90 °C h^{-1} with a 15 min pre-scan thermostating. For each GdnHCl concentration, a buffer baseline was obtained, and protein thermograms were obtained after subtracting the buffer baseline using Origin software (Originlab Corporation, Northampton, MA). For each concentration of GdnHCl tested, three vials of protein solution were prepared and analyzed.

RESULTS

Far-UV CD Spectrum and Unfolding Curve for mAb. To examine the mAb secondary structure, far-UV CD spectra (Figure 1A) for mAb at 1 mg mL^{-1} were obtained. A minimum was observed at 218 nm, likely dominated by contributions from β-sheet structure.[70,71] Mean residue ellipticity at 218 nm was plotted as a function of GdnHCl concentration (Figure 1B), which showed an onset of protein unfolding at 1.8 M GdnHCl.

Spectroscopic Characterization of Partially Unfolded Protein Species. To obtain insight into protein conformation prior to aggregation, intrinsic tryptophan (Trp) fluorescence and CD spectra were obtained on the day of preparation (day 0) and after 24 h of incubation at 37 °C.

The wavelengths for maximum tryptophan fluorescence (λ_{max}) were plotted as a function of GdnHCl concentration (Figure 2A). It is important to note that this mAb contains 22 Trp residues and thus the Trp fluorescence reflects an average over all fluorescing Trp residues. In the absence of GdnHCl, λ_{max} for the native mAb occurred around 330 nm. This

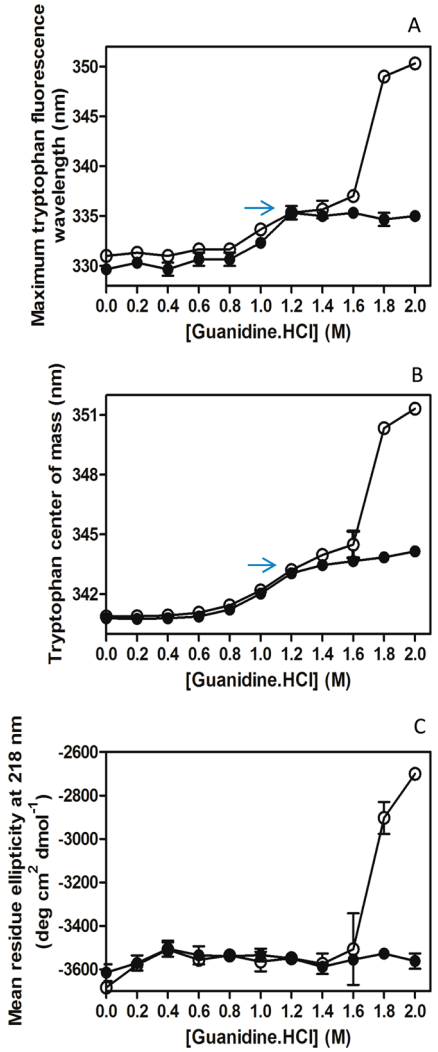

Figure 2. (A) Maximum tryptophan fluorescence wavelength for the mAb on day 0 (closed circles) and day 1 (open circles). (B) Tryptophan center of mass for mAb on day 0 (closed circles) and day 1 (open circles). (C) CD signal observed for the mAb on day 0 (closed circles) and day 1 (open circles). Data points represent the mean ± SD for triplicate samples. Error bars for certain data points are smaller than their associated symbols.

indicates that most of the fluorescing tryptophans are buried in the hydrophobic interior of the protein.[72] In solutions

dx.doi.org/10.1021/bi5002163 | *Biochemistry* 2014, 53, 3367−3377

containing 0−0.8 M GdnHCl, λ_{max} did not shift appreciably, but it increased by ca. 5 nm at GdnHCl concentrations ranging from 1.2 to 1.6 M, indicating a moderate perturbation in the mAb tertiary structure. At day 0, λ_{max} was around 335 nm for samples containing 1.2−2.0 M GdnHCl. On day 1, λ_{max} values measured in samples containing 0−1.6 M GdnHCl were very similar to those observed on day 0, but λ_{max} increased to 350 nm at GdnHCl concentrations of 1.8 and 2.0 M. This increase in λ_{max} reflects an average increase in the exposure of fluorescing Trp residues to an aqueous environment and is thus indicative of a major perturbation of tertiary structure.[17]

We also calculated the tryptophan fluorescence center of mass for the same set of samples (Figure 2B). The trend observed was similar to that for the maximum tryptophan fluorescence wavelengths plotted in Figure 2A. However, because of the asymmetrical peak shape, this analysis resulted in an apparent 10 nm red shift in the reported peak position.[73]

In an attempt to obtain further insights into changes in tertiary structure, near-UV-CD spectroscopy was also used to analyze the same set of samples. However, unlike fluorescence spectra, near-UV-CD spectra did not show changes (data not shown) indicative of tertiary structure perturbations until GdnHCl was at concentrations at which there were also secondary structure alterations.

To study secondary structure, mean residue ellipticities at 218 nm determined from far-UV-CD spectra were plotted as a function of GdnHCl (Figure 2C). On days 0 and 1, only a small decrease in signal intensity was observed as up to 0.4 M GdnHCl was added to mAb samples, with no further intensity changes in day 0 samples with up to 2.0 M GdnHCl. In contrast, after a day of incubation, there was a dramatic decrease in intensity at 1.8 and 2.0 M GdnHCl (Figure 2C), indicating perturbation of the mAb secondary structure.

On days 0 and 1, tertiary structure of the mAb was perturbed in the presence of 1.2, 1.4, and 1.6 M GdnHCl (Figure 2A), but secondary structure appeared to be largely unaffected (Figure 2C). However, in 1.8 and 2.0 M GdnHCl on day 1, concomitant large perturbations of both tertiary and secondary structure were observed. It important to note that protein aggregation was not observed for any of the samples on days 0 and 1 (see below). Thus, the spectroscopic results reflect alteration in protein structure prior to any aggregation.

Protein−Protein Interactions. B_{22} values normalized by the hard sphere value for the mAb are shown as a function of GdnHCl in Figure 3. For protein incubated in 0−2.0 M, the normalized B_{22} values are negative, indicating that the protein−protein interactions are attractive in these concentration ranges.[44]

Characterization of Soluble Aggregates. *Size-Exclusion Chromatography.* mAb samples incubated in 0−2.0 M GdnHCl at 37 °C over a period of 11 days were analyzed for soluble protein and high-molecular-weight species by SEC (Figure 4). There were no significant losses of soluble protein during the incubation period (Figure 4A). No soluble aggregates were observed by SEC on days 0 and 1 (Figure 4B). After 6 days of incubation at 37 °C, high-molecular-weight species were observed in samples containing 1.2, 1.4, 1.6, and 1.8 M GdnHCl (Figure 4B), with additional increases seen by day 11. In contrast, no aggregates were detected for mAb samples in 0−1.0 and 2.0 M GdnHCl, even after 11 days of incubation.

Dynamic Light Scattering. To further characterize the soluble aggregates, DLS was used to measure mAb hydrodynamic diameters in samples after incubation at 37 °C (Figure 5). On day 0, before aggregates were detected by SEC, the hydrodynamic diameter of mAb in 0−2.0 M GdnHCl was ca. 11 nm. On day 1, the average hydrodynamic diameter increased to ca. 15 nm in solutions containing 1.4 M and greater concentrations of GdnHCl. This increase may have resulted from unfolding of the mAb and/or formation of small amount of aggregates. Consistent with results from SEC analysis that showed formation of soluble aggregates, after 6 days of incubation the measured hydrodynamic diameter increased dramatically in samples incubated in 1.2−2.0 M GdnHCl, with a maximum of about 28 nm observed in samples incubated in 1.4 and 1.6 M GdnHCl. A similar trend was observed on day 11.

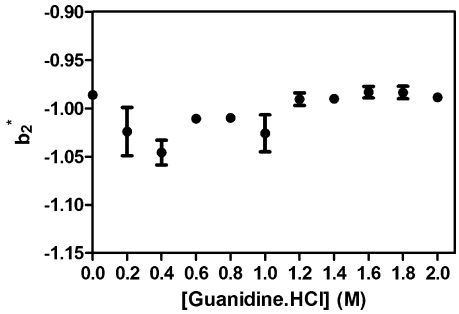

Figure 3. Second osmotic virial coefficient, B_{22}, normalized by the B_{22} value for a hard sphere ($B_{22}/B_{22}^{HS} - 1$) gives value of b_2* as a function of GdnHCl for mAb. Data points represent the mean ± SD for triplicate samples. Error bars for certain data points are smaller than their associated symbols.

Sedimentation Velocity Analytical Ultracentrifugation. mAb samples incubated in 0−2.0 M GdnHCl were analyzed by AUC to determine the levels of high-molecular-weight species (Figure 6). The AUC results showed trends identical to those observed with SEC and DLS.

Far-UV CD Spectroscopy of Incubated mAb Samples. Far-UV CD spectroscopy was used to analyze changes in the secondary structure of mAb upon formation of soluble aggregates in incubated samples (Figure 7). After 6 and 11 days, mean residue ellipticity measured at 218 nm became more negative for samples incubated in 1.4 and 1.6 M GdnHCl, reflecting the characteristic intermolecular β-sheet structure that is typical of protein aggregates.[74] In samples incubated in 1.8 and 2.0 M GdnHCl, mAb unfolding occurred, as evidenced by less negative ellipticity values.

Percent Covalent Aggregates by SDS-PAGE Analysis. The total percentage of protein that formed covalent aggregates was quantified by SDS-PAGE analysis (Figure 8). Protein in 1.4 M and greater concentrations of GdnHCl showed covalent aggregates. However, these covalent aggregates were only a fraction of the total amount of aggregates observed for these samples (Figures 4, 6, and 8).

We also tested for the presence of free cysteines in the mAb using Ellman's reagent.[75] The Ellman's reagent test did not show the presence of free thiols (data not shown); we suggest that covalent aggregates were formed from disulfide shuffling within existing aggregates.

Proteinase K Assay. Proteinase K assay was used to determine proteolytic digestion pattern for mAb in various concentrations of GdnHCl on days 0 and 1 (Figure 9). The band at ∼50 kDa corresponds to the mAb's heavy chain, and the band at ∼25 kDa corresponds to the light chain. For

dx.doi.org/10.1021/bi5002163 | Biochemistry 2014, 53, 3367−3377

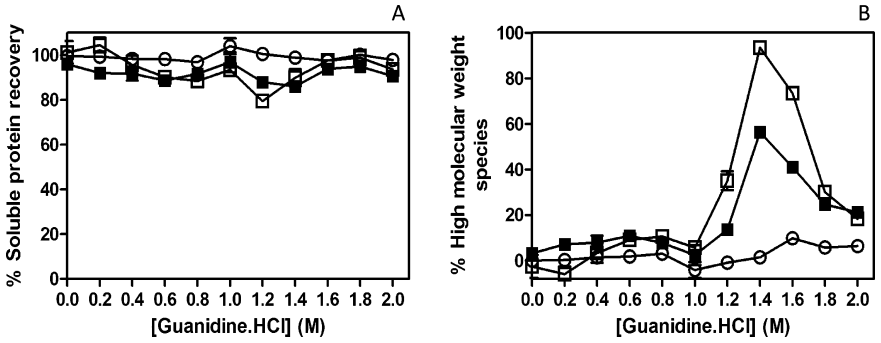

Figure 4. (A) Percent soluble protein recovery as determined by size-exclusion chromatography (SEC) relative to day 0. (B) Percent high-molecular-weight species observed using SEC relative to day 0. Open circles represent day 1 samples, closed squares represent day 6 samples, and open squares represent day 11 samples. Data points represent the mean ± SD for triplicate samples. Error bars for certain data points are smaller than their associated symbols.

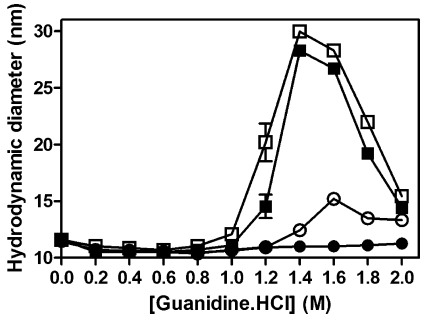

Figure 5. Average size of soluble protein as observed using dynamic light scattering (DLS). Closed circles represent day 0 samples, open circles represent day 1 samples, closed squares represent day 6 samples, and open squares represent day 11 samples. Data points represent the mean ± SD for triplicate samples. Error bars for certain data points are smaller than their associated symbols.

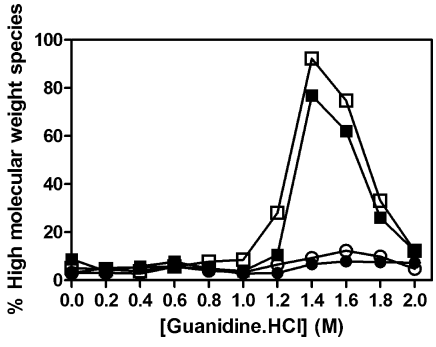

Figure 6. Percent aggregates as observed using analytical ultracentrifugation (AUC). Closed circles represent day 0 samples, open circles represent day 1 samples, closed squares represent day 6 samples, and open squares represent day 11 samples.

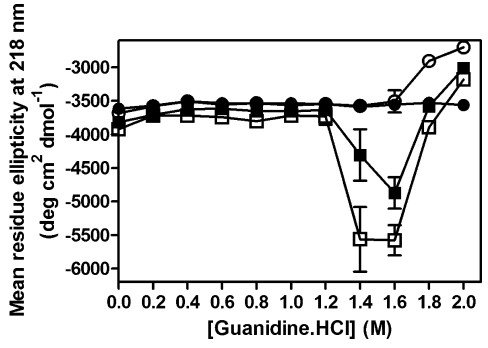

Figure 7. Mean residue ellipticity at 218 nm for incubated samples. Closed circles represent day 0 samples, open circles represent day 1 samples, closed squares represent day 6 samples, and open squares represent day 11 samples. Data points represent the mean ± SD for triplicate samples. Error bars for certain data points are smaller than their associated symbols.

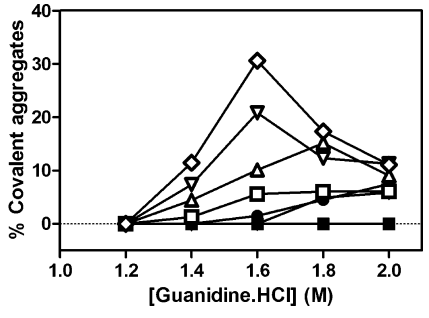

Figure 8. Percent covalent aggregates for mAb as a function of GdnHCl concentration. Solid squares represent day 0 samples, solid triangles represent day 0.5 samples, solid inverted triangles represent day 1 samples, solid diamonds represent day 1.5 samples, solid circles represent day 2 samples, open squares represent day 3 samples, open triangles represent day 4 samples, open inverted triangles represent day 6 samples, and open diamonds represent day 11 samples.

samples digested by proteinase K on day 0, the intensity of the band for the heavy chain decreased with increasing concentration of GdnHCl, and the band disappeared entirely in samples containing 1.0−2.0 M. In contrast, the presence of GdnHCl across the entire range tested (0−2.0 M) did not appear to affect the intensity of the band for the light chain. For day 1 samples, the heavy chain band exhibited a similar trend, but in samples containing 1.6−2.0 M GdnHCl, the light chain band was greatly diminished.

It should be pointed out that TCA precipitation of the mAb in the absence of GdnHCl or proteinase K led to formation of covalent aggregates (lane 2). In contrast, no such aggregates were observed when the protein was analyzed by SDS-PAGE in the absence of TCA precipitation (Figure 9C).

Hydrodynamic Behavior of Protein in 0−2.0 M GdnHCl. Sedimentation velocity analytical ultracentrifugation (SV-AUC) was used to determine sedimentation coefficients corrected for standard conditions ($s_{20,w}$) for the mAb in 0−2.0 M GdnHCl (Table 1). In 0 M GdnHCl, the mAb had a sedimentation coefficient of 7.3 S both on day 0 and day 1. The value of

dx.doi.org/10.1021/bi5002163 | *Biochemistry* 2014, 53, 3367−3377

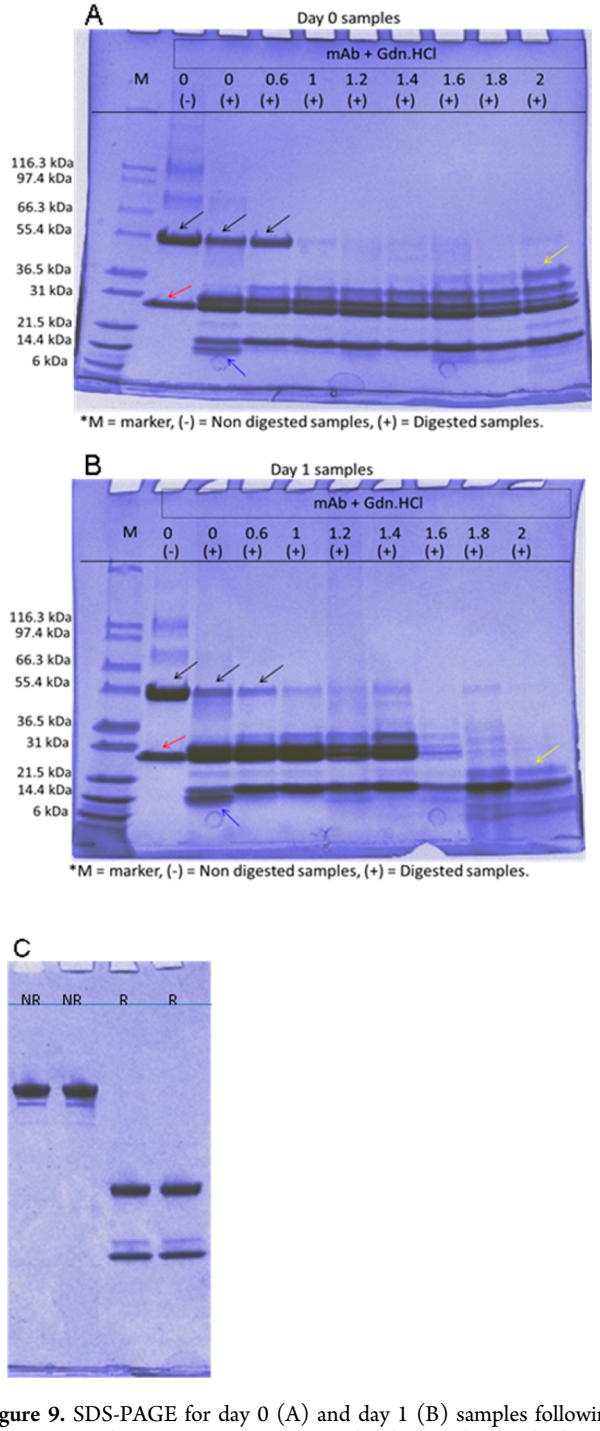

Figure 9. SDS-PAGE for day 0 (A) and day 1 (B) samples following proteinase K digestion. M represents molecular weight standards, and the number corresponds to a particular concentration of GdnHCl. Samples marked "+" are digested samples and "−" are the nondigested samples. (C) mAb samples in nonreduced (NR) and reduced (R) forms without TCA precipitation.

sedimentation coefficient decreased with increasing concentrations of GdnHCl. This trend is apparent on day 0 as well as day 1.

DSC To Observe mAb Domain Unfolding Transitions. DSC analysis was used to obtain information about domain unfolding in 0−2.0 M GdnHCl solutions. The native protein showed three thermal unfolding transitions (T_m) (Figure 10). The first transition ($T_{m,1}$) observed at around 48.9 °C can be attributed to unfolding of the C_H2 domain.[76] The second and third transitions ($T_{m,2}$ and $T_{m,3}$) observed at around 72.1 and 84.5 °C can be attributed to the F_{ab} region and C_H3 regions of the mAb, respectively.[76] In 1.4 M GdnHCl, the first transition ($T_{m,1}$) was not detected, suggesting that the C_H2 domain was unfolded prior to heating. Also, the other two transitions ($T_{m,2}$ and $T_{m,3}$) shifted to lower temperatures, indicating that the presence of 1.4 M GdnHCl reduced the stability of the C_H3 and Fab domains.

In solutions containing 0−2.0 M GdnHCl, $T_{m,2}$ and $T_{m,3}$ values decreased with increasing concentrations of GdnHCl. For $T_{m,1}$, a decrease was observed from 0 to 1.0 M GdnHCl, but no transition could be detected in 1.2−2.0 M GdnHCl.

Table 1. Sedimentation Coefficient for a Monomer of mAb as a Function of GdnHCl on Days 0 and 1 of Incubation[a]

[GdnHCl]	$s_{20,w}$ (day 0)	$s_{20,w}$ (day 1)
0	7.3	7.3
0.2	6.3	6.3
0.4	6.1	6.1
0.6	6.0	6.0
0.8	5.7	5.7
1	5.5	5.5
1.2	5.3	5.3
1.4	5.1	4.9
1.6	4.9	4.6
1.8	4.8	4.6
2	4.6	4.3

[a]Note: hydrodynamic size of mAb is time-dependent at higher concentrations of GdnHCl.

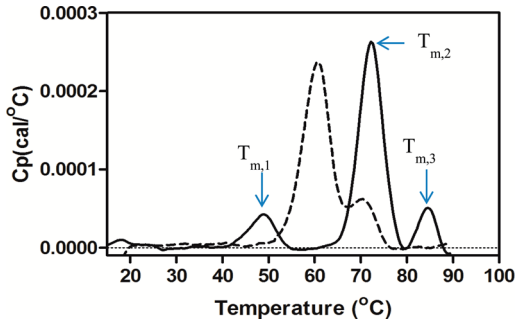

Figure 10. DSC thermograms for native mAb (solid black line) and mAb in the presence of 1.4 M GdnHCl (dashed black line). The native mAb shows three transitions marked as $T_{m,1}$, $T_{m,2}$, and $T_{m,3}$.

DISCUSSION

Partially Unfolded Protein Species as a Constituent of Protein Ensemble. Hydrogen−deuterium exchange and NMR relaxation studies have revealed significant conformational heterogeneity of protein molecules under native-state conditions.[27,77,78] The ensemble of native protein molecules has access to diverse conformations, which may be critical for biological function.[79] Also included in the native-state ensemble may be partially unfolded protein species that are prone to aggregation.[77,79]

The levels of these partially unfolded states (and hence the resulting rates of aggregation) can be modified within the native-state ensemble by changes in the solution conditions. For example, the presence of low concentrations of GdnHCl results in accumulation of partially unfolded protein molecules[34,51,52] that tend to aggregate.[53] We found that the large, multidomain mAb became partially unfolded with unfolding of

dx.doi.org/10.1021/bi5002163 | Biochemistry 2014, 53, 3367−3377

the C_H2 domain at low concentrations of GdnHCl, which in turn resulted in aggregation.

Conformational and Colloidal Instability Govern Protein Aggregation. Protein aggregation can be controlled by both the conformational state of a protein and the energetics of protein−protein intermolecular interactions.[6,58] Early studies of protein aggregation focused on the role of protein conformation in the aggregation process.[13,15,35] Many reports[6,18] have shown that protein aggregation proceeds via assembly of partially unfolded protein molecules. These species can be populated under a variety of conditions, including elevated temperatures, pH extremes, exposure to interfaces, presence of low levels of chemical denaturants, and freeze−thawing.[13,30,80−87]

For large proteins that have multiple domains, the analysis of overall protein stability is a complicated process because each individual domain contributes to stability. It has been suggested that the stability of the least stable protein domain will dominate the conformational stability of a protein toward aggregation.[40] Also, the reversibility of unfolded regions of a multidomain protein may be unfavorable, often leading to aggregation.[88] Furthermore, the overall protein structure is stabilized by both inter- and intradomain interactions.[89,90]

The mAb investigated in the current study consists of 12 domains. Because partially unfolded molecules of this protein are involved in aggregation, we expected that the least stable doman will unfold at lower concentrations of GdnHCl than other domains and lead to aggregation. It has been shown that mutations in this particular mAb reduced only the stability of the C_H2 domain and led to increased aggregation compared to the that of the wild-type protein.[76] Similarly, in our DSC study, we observed that the unfolding transition corresponding to the C_H2 domain was not detected for protein in 1.2 M and higher concentrations of GdnHCl (Figure 10 and Table 2). Thus, it can be suggested that unfolding of the C_H2 domain of the mAb resulted in partially unfolded species for this protein, which in turn were prone to aggregation. Other studies carried out on mAb have also reported that the C_H2 domain can play a causal role in aggregation.[38,39,81,91]

Table 2. Thermal Unfolding Transitions (T_m) for mAb in Sub-Denaturing Concentrations of GdnHCl as Measured by DSC[a]

[GdnHCl]	$T_{m,1}$ (°C)	$T_{m,2}$ (°C)	$T_{m,3}$ (°C)
0	48.6 ± 0.2	72.1 ± 0.0	84.2 ± 0.2
0.2	49.0 ± 0.2	73.2 ± 0.3	79.1 ± 0.7
0.4	46.1 ± 0.4	75.1 ± 0.3	80.5 ± 0.6
0.6	42.1 ± 0.3	67.4 ± 0.4	73.5 ± 0.6
0.8	37.9 ± 0.2	66.3 ± 0.3	74.4 ± 0.2
1	35.0 ± 3.9	64.7 ± 0.4	73.9 ± 0.6
1.2	ND	62.5 ± 0.1	71.9 ± 0.2
1.4	ND	61.0 ± 0.2	71.0 ± 0.9
1.6	ND	59.2 ± 0.2	68.8 ± 0.7
1.8	ND	57.1 ± 0.1	66.7 ± 0.5
2	ND	54.9 ± 0.2	65.6 ± 0.6

[a]ND signifies that the transition ($T_{m,1}$) was not observed for that particular sample. Each number represents the mean transition temperature (T_m) and the standard deviation of triplicate measurements.

We also found that the S value obtained from sedimentation velocity experiments was inversely proportional to hydrodynamic radius of the protein. As the concentration of denaturant increased, the S value became smaller, signifying a a larger hydrodynamic radius of the protein (Table 1). We also observe that the S value for protein in 1.2−1.6 M GdnHCl is intermediate for that of native protein and that observed in 2.0 M GdnHCl. This observation further supports the conclusion that protein in 1.2−1.6 M GdnHCl was partially unfolded.

Partially unfolded protein species have structurally perturbed regions that are more susceptible to proteolytic cleavage than the structured regions.[92] Studies have shown that proteolytic enzymes can be used as probes of the structure and dynamics of partially folded states of protein and that the residual native structure of the protein molecule can be sufficient to prevent extensive proteolysis.[93] Some reports have depicted that altering solution conditions to increase the population of unfolded molecules results in increased proteolysis.[68] For example, Latypov et al. showed using proteinase K that in 4 M urea, IL-1ra was resistant to proteolysis and only 25% molecules were digested.[69] However, 90% of IL-1ra molecules were digested in 5 M urea.[69] We found that the mAb was more susceptible to proteolysis in 2 M GdnHCl (Figure 9B) than in buffer alone because in the denaturant the protein molecules were mostly present in an unfolded state. However, the susceptibility of partially unfolded species in 1.2−1.6 M GdnHCl to proteolysis was intermediate to that of the folded and unfolded states. Overall, the heavy chain was more susceptible to proteolysis than the light chain of this mAb, as observed from Figure 9. For samples digested by proteinase K on day 0, the intensity of the band for the heavy chain decreased with increasing concentration of GdnHCl, and the band disappeared entirely in samples containing 1.0−2.0 M. In contrast, the presence of GdnHCl across the entire range tested (0−2.0 M) did not appear to affect the intensity of the band for the light chain. A similar trend was observed for day 1 samples as well, with the light chain getting digested further for samples containing 1.6−2.0 M GdnHCl. This trend indicates unfolding of protein in higher concentrations of GdnHCl.

Colloidal instability relates to intermolecular interactions leading to aggregation. Under solution conditions where protein molecules experience net attractive interaction energies, assembly into aggregated species is favored. Under these conditions, there may or may not be an associated change in protein conformation.[6] Earlier studies have shown that protein−protein interactions are most attractive at low concentrations of GdnHCl.[94,95] For some proteins, colloidal instabilities control rates of aggregation.[58] In our study, we found that colloidal stability was not a dominating factor in the overall process of aggregation. Despite b_2* being negative for protein in 0−2.0 M GdnHCl, no aggregates were observed for mAb samples incubated in 0−1.0 M GdnHCl (Figure 3). Aggregates were only observed for protein in 1.2 M and higher concentrations of GdnHCl, where tertiary structure was perturbed (Figure 2), and led to C_H2 domain unfolding (Figure 10). Thus, with this particular mAb, conformational perturbations caused by GdnHCl that lead to aggregation do not also cause a change in colloidal stability. Thus, conformation stability is dominant over colloidal stability in governing the aggregation process for the mAb.

Characterization of mAb Aggregates. An increased level of intermolecular β-sheet is a common feature of protein aggregates.[13] The structural transition of native protein to form non-native intermolecular β-sheet structures can occur regardless of the initial secondary structural composition.[6]

dx.doi.org/10.1021/bi5002163 | Biochemistry 2014, 53, 3367−3377

For instance, aggregation of protein molecules like rhIFN-γ and prion proteins results in intermolecular β-sheet structure concomintant with a significant loss of α-helix.[96,97] Although secondary structure of native mAb molecules is about 70% β-sheet,[89] aggregation of the mAb used in this study (Figure 7) and earlier research resulted in an increase in β-sheet content.[98] The high β-sheet content may also reflect the retention of intact, native-like domains of the mAb molecules within the aggregate.[43,99] Overall, it appears that the aggregation-prone, partially unfolded molecules retained native-like β-sheet secondary structure based on CD spectroscopy (Figure 2A) despite having an unfolded C_H2 domain. In addition, upon aggregate formation there was an increase in non-native β-sheet because of additional structural perturbation as a result of aggregation.

We also investigated the potential for the aggregates of the mAb to have covalent intermolecular contacts. We found that there were no free thiols in this mAb under different concentrations of GdnHCl. However, upon further incubation, intermolecular disulfide bonds were formed, making the aggregates irreversible. These results suggest that in addition to structural perturbation occurring initially upon aggregate formation, there are structural changes in the mAb molecules in the aggregate that allow non-native intermolecular disulfide bonds to form. Such formation of covalent links between protein molecules in aggregates has been observed for other proteins.[100−102]

CONCLUSIONS

We observed that the b_2* values were negative for the mAb molecules over the entire range of 0−2 M GdnHCl. However, aggregation was only observed for samples at 1.2 M and higher concentrations of GdnHCl. Therefore, colloidal stability does not control aggregation of this mAb. Rather, at 1.2 M and higher concentrations of the chaotrope, the C_H2 domains of the mAb were unfolded, resulting in a population of partially unfolded, aggregation-prone protein molecules. Thus, for this mAb, conformational perturbation predominately controlled the rates of aggregation.

AUTHOR INFORMATION

Corresponding Author

*Phone: 303-724-6110. Fax: 303-724-7266. E-mail: John.Carpenter@UCDenver.edu.

Notes

The authors declare no competing financial interest.

REFERENCES

(1) Hardy, J., and Gwinn-Hardy, K. (1998) Genetic classification of primary neurodegenerative disease. *Science 282*, 1075−1079.

(2) Harper, J. D., and Lansbury, P. T., Jr. (1997) Models of amyloid seeding in Alzheimer's disease and scrapie: mechanistic truths and physiological consequences of the time-dependent solubility of amyloid proteins. *Annu. Rev. Biochem. 66*, 385−407.

(3) Koo, E. H., Lansbury, P. T., Jr., and Kelly, J. W. (1999) Amyloid diseases: abnormal protein aggregation in neurodegeneration. *Proc. Natl. Acad. Sci. U.S.A. 96*, 9989−9990.

(4) Kyle, R. A. (1994) Monoclonal proteins and renal disease. *Annu. Rev. Med. 45*, 71−77.

(5) Lansbury, P. T., Jr. (1999) Evolution of amyloid: what normal protein folding may tell us about fibrillogenesis and disease. *Proc. Natl. Acad. Sci. U. S. A. 96*, 3342−3344.

(6) Chi, E. Y., Krishnan, S., Randolph, T. W., and Carpenter, J. F. (2003) Physical stability of proteins in aqueous solution: mechanism and driving forces in nonnative protein aggregation. *Pharm. Res. 20*, 1325−1336.

(7) Wang, W. (2005) Protein aggregation and its inhibition in biopharmaceutics. *Int. J. Pharm. 289*, 1−30.

(8) Moore, W. V., and Leppert, P. (1980) Role of aggregated human growth hormone (hGH) in development of antibodies to hGH. *J. Clin. Endocrinol. Metab. 51*, 691−697.

(9) Ratner, R. E., Phillips, T. M., and Steiner, M. (1990) Persistent cutaneous insulin allergy resulting from high-molecular-weight insulin aggregates. *Diabetes 39*, 728−733.

(10) Thornton, C. A., and Ballow, M. (1993) Safety of intravenous immunoglobulin. *Arch. Neurol. 50*, 135−136.

(11) Manning, M. C., Patel, K., and Borchardt, R. T. (1989) Stability of protein pharmaceuticals. *Pharm. Res. 6*, 903−918.

(12) Cleland, J. F., Powell, M. F., and Shire, S. J. (1993) *Crit. Rev. Ther. Drug Carrier Syst.*, 307−377.

(13) Dong, A., Prestrelski, S. J., Allison, S. D., and Carpenter, J. F. (1995) Infrared spectroscopic studies of lyophilization- and temperature-induced protein aggregation. *J. Pharm. Sci. 84*, 415−424.

(14) De Young, L. R., Dill, K. A., and Fink, A. L. (1993) Aggregation and denaturation of apomyoglobin in aqueous urea solutions. *Biochemistry 32*, 3877−3886.

(15) Lumry, R., and Eyring, E. (1954) Conformation changes of proteins. *J. Phys. Chem. 58*, 110−120.

(16) Khurana, R., Gillespie, J. R., Talapatra, A., Minert, L. J., Ionescu-Zanetti, C., Millett, I., and Fink, A. L. (2001) Partially folded intermediates as critical precursors of light chain amyloid fibrils and amorphous aggregates. *Biochemistry 40*, 3525−3535.

(17) Fink, A. L. (1998) Protein aggregation: folding aggregates, inclusion bodies and amyloid. *Folding Des. 3*, R9−23.

(18) Fink, A. L., Calciano, L. J., Goto, Y., Kurotsu, T., and Palleros, D. R. (1994) Classification of acid denaturation of proteins: intermediates and unfolded states. *Biochemistry 33*, 12504−12511.

(19) Carrotta, R., Bauer, R., Waninge, R., and Rischel, C. (2001) Conformational characterization of oligomeric intermediates and aggregates in beta-lactoglobulin heat aggregation. *Protein Sci. 10*, 1312−1318.

(20) Gomez-Orellana, I., Variano, B., Miura-Fraboni, J., Milstein, S., and Paton, D. R. (1998) Thermodynamic characterization of an intermediate state of human growth hormone. *Protein Sci. 7*, 1352−1358.

(21) Speed, M. A., Morshead, T., Wang, D. I., and King, J. (1997) Conformation of P22 tailspike folding and aggregation intermediates probed by monoclonal antibodies. *Protein Sci. 6*, 99−108.

(22) King, J., Haase-Pettingell, C., Robinson, A. S., Speed, M., and Mitraki, A. (1996) Thermolabile folding intermediates: inclusion body precursors and chaperonin substrates. *FASEB J. 10*, 57−66.

(23) Kim, D., and Yu, M. H. (1996) Folding pathway of human alpha 1-antitrypsin: characterization of an intermediate that is active but prone to aggregation. *Biochem. Biophys. Res. Commun. 226*, 378−384.

(24) Grillo, A. O., Edwards, K. L., Kashi, R. S., Shipley, K. M., Hu, L., Besman, M. J., and Middaugh, C. R. (2001) Conformational origin of the aggregation of recombinant human factor VIII. *Biochemistry 40*, 586−595.

(25) Whitten, S. T., Kurtz, A. J., Pometun, M. S., Wand, A. J., and Hilser, V. J. (2006) Revealing the nature of the native state ensemble through cold denaturation. *Biochemistry 45*, 10163−10174.

(26) Englander, S. W. (2000) Protein folding intermediates and pathways studied by hydrogen exchange. *Annu. Rev. Biophys. Biomol. Struct. 29*, 213−238.

(27) Chamberlain, A. K., Handel, T. M., and Marqusee, S. (1996) Detection of rare partially folded molecules in equilibrium with the native conformation of RNaseH. *Nat. Struct. Biol. 3*, 782−787.

(28) Singh, S. M., Cabello-Villegas, J., Hutchings, R. L., and Mallela, K. M. (2010) Role of partial protein unfolding in alcohol-induced protein aggregation. *Proteins 78*, 2625−2637.

(29) Alford, J. R., Fowler, A. C., Wuttke, D. S., Kerwin, B. A., Latypov, R. F., Carpenter, J. F., and Randolph, T. W. (2011) Effect of benzyl alcohol on recombinant human interleukin-1 receptor

antagonist structure and hydrogen-deuterium exchange. *J. Pharm. Sci. 100*, 4215−4224.
(30) Roy, S., Katayama, D., Dong, A., Kerwin, B. A., Randolph, T. W., and Carpenter, J. F. (2006) Temperature dependence of benzyl alcohol- and 8-anilinonaphthalene-1-sulfonate-induced aggregation of recombinant human interleukin-1 receptor antagonist. *Biochemistry 45*, 3898−3911.
(31) Zhang, Y., Roy, S., Jones, L. S., Krishnan, S., Kerwin, B. A., Chang, B. S., Manning, M. C., Randolph, T. W., and Carpenter, J. F. (2004) Mechanism for benzyl alcohol-induced aggregation of recombinant human interleukin-1 receptor antagonist in aqueous solution. *J. Pharm. Sci. 93*, 3076−3089.
(32) Thirumangalathu, R., Krishnan, S., Brems, D. N., Randolph, T. W., and Carpenter, J. F. (2006) Effects of pH, temperature, and sucrose on benzyl alcohol-induced aggregation of recombinant human granulocyte colony stimulating factor. *J. Pharm. Sci. 95*, 1480−1497.
(33) Fink, A. L., Oberg, K. A., and Seshadri, S. (1998) Discrete intermediates versus molten globule models for protein folding: characterization of partially folded intermediates of apomyoglobin. *Folding Des. 3*, 19−25.
(34) Mayo, S. L., and Baldwin, R. L. (1993) Guanidinium chloride induction of partial unfolding in amide proton exchange in RNase A. *Science 262*, 873−876.
(35) Raso, S. W., Abel, J., Barnes, J. M., Maloney, K. M., Pipes, G., Treuheit, M. J., King, J., and Brems, D. N. (2005) Aggregation of granulocyte-colony stimulating factor in vitro involves a conformationally altered monomeric state. *Protein Sci. 14*, 2246−2257.
(36) Seefeldt, M. B., Kim, Y. S., Tolley, K. P., Seely, J., Carpenter, J. F., and Randolph, T. W. (2005) High-pressure studies of aggregation of recombinant human interleukin-1 receptor antagonist: thermodynamics, kinetics, and application to accelerated formulation studies. *Protein Sci. 14*, 2258−2266.
(37) Souillac, P. O. (2005) Biophysical characterization of insoluble aggregates of a multi-domain protein: an insight into the role of the various domains. *J. Pharm. Sci. 94*, 2069−2083.
(38) Majumdar, R., Manikwar, P., Hickey, J. M., Samra, H. S., Sathish, H. A., Bishop, S. M., Middaugh, C. R., Volkin, D. B., and Weis, D. D. (2013) Effects of salts from the Hofmeister series on the conformational stability, aggregation propensity, and local flexibility of an IgG1 monoclonal antibody. *Biochemistry. 52*, 3376−3389.
(39) Andersen, C. B., Manno, M., Rischel, C., Thorolfsson, M., and Martorana, V. (2010) Aggregation of a multidomain protein: a coagulation mechanism governs aggregation of a model IgG1 antibody under weak thermal stress. *Protein Sci. 19*, 279−290.
(40) Fast, J. L., Cordes, A. A., Carpenter, J. F., and Randolph, T. W. (2009) Physical instability of a therapeutic Fc fusion protein: domain contributions to conformational and colloidal stability. *Biochemistry 48*, 11724−11736.
(41) Cordes, A. A., Platt, C. W., Carpenter, J. F., and Randolph, T. W. (2012) Selective domain stabilization as a strategy to reduce fusion protein aggregation. *J. Pharm. Sci. 101*, 1400−1409.
(42) Cordes, A. A., Carpenter, J. F., and Randolph, T. W. (2012) Selective domain stabilization as a strategy to reduce human serum albumin−human granulocyte colony stimulating factor aggregation rate. *J. Pharm. Sci. 101*, 2009−2016.
(43) Rousseau, F., Schymkowitz, J. W., and Itzhaki, L. S. (2003) The unfolding story of three-dimensional domain swapping. *Structure 11*, 243−251.
(44) Brummitt, R. K., Nesta, D. P., Chang, L., Chase, S. F., Laue, T. M., and Roberts, C. J. (2011) Nonnative aggregation of an IgG1 antibody in acidic conditions: Part 1. Unfolding, colloidal interactions, and formation of high-molecular-weight aggregates. *J. Pharm. Sci. 100*, 2087−2103.
(45) Arosio, P., Jaquet, B., Wu, H., and Morbidelli, M. (2012) On the role of salt type and concentration on the stability behavior of a monoclonal antibody solution. *Biophys. Chem. 168−169*, 19−27.
(46) Gerhardt, A., Bonam, K., Bee, J. S., Carpenter, J. F., and Randolph, T. W. (2013) Ionic strength affects tertiary structure and aggregation propensity of a monoclonal antibody adsorbed to silicone oil-water interfaces. *J. Pharm. Sci. 102*, 429−440.
(47) Kim, N., Remmele, R. L., Jr., Liu, D., Razinkov, V. I., Fernandez, E. J., and Roberts, C. J. (2013) Aggregation of anti-streptavidin immunoglobulin gamma-1 involves Fab unfolding and competing growth pathways mediated by pH and salt concentration. *Biophys Chem. 172*, 26−36.
(48) Dyson, H. J., and Wright, P. E. (1998) Equilibrium NMR studies of unfolded and partially folded proteins. *Nat. Struct. Biol. 5*, 499−503.
(49) Matthews, C. R. (1993) Pathways of protein folding. *Annu. Rev. Biochem. 62*, 653−683.
(50) Greene, R. F., Jr., and Pace, C. N. (1974) Urea and guanidine hydrochloride denaturation of ribonuclease, lysozyme, alpha-chymotrypsin, and beta-lactoglobulin. *J. Biol. Chem. 249*, 5388−5393.
(51) Srimathi, T., Kumar, T. K., Chi, Y. H., Chiu, I. M., and Yu, C. (2002) Characterization of the structure and dynamics of a near-native equilibrium intermediate in the unfolding pathway of an all beta-barrel protein. *J. Biol. Chem. 277*, 47507−47516.
(52) Samuel, D., Kumar, T. K., Srimathi, T., Hsieh, H., and Yu, C. (2000) Identification and characterization of an equilibrium intermediate in the unfolding pathway of an all beta-barrel protein. *J. Biol. Chem. 275*, 34968−34975.
(53) Qin, Z., Hu, D., Zhu, M., and Fink, A. L. (2007) Structural characterization of the partially folded intermediates of an immunoglobulin light chain leading to amyloid fibrillation and amorphous aggregation. *Biochemistry 46*, 3521−3531.
(54) De Bernardez Clark, E., Hevehan, D., Szela, S., and Maachupalli-Reddy, J. (1998) Oxidative renaturation of hen egg-white lysozyme. Folding vs aggregation. *Biotechnol. Prog. 14*, 47−54.
(55) Maachupalli-Reddy, J., Kelley, B. D., and De Bernardez Clark, E. (1997) Effect of inclusion body contaminants on the oxidative renaturation of hen egg white lysozyme. *Biotechnol. Prog. 13*, 144−150.
(56) Goldberg, M. E., Rudolph, R., and Jaenicke, R. (1991) A kinetic study of the competition between renaturation and aggregation during the refolding of denatured-reduced egg white lysozyme. *Biochemistry 30*, 2790−2797.
(57) Ho, J. G., Middelberg, A. P., Ramage, P., and Kocher, H. P. (2003) The likelihood of aggregation during protein renaturation can be assessed using the second virial coefficient. *Protein Sci. 12*, 708−716.
(58) Chi, E. Y., Krishnan, S., Kendrick, B. S., Chang, B. S., Carpenter, J. F., and Randolph, T. W. (2003) Roles of conformational stability and colloidal stability in the aggregation of recombinant human granulocyte colony-stimulating factor. *Protein Sci. 12*, 903−913.
(59) George, A., and Wilson, W. W. (1994) Predicting protein crystallization from a dilute solution property. *Acta Crystallogr., Sect. D: Biol. Crystallogr. 50*, 361−365.
(60) Muschol, M., and Rosenberger, F. (1995) Interactions in undersaturated and supersaturated lysozyme solutions: Static and dynamic light scattering results. *J. Chem. Phys. 103*, 10424.
(61) Pace, C. N. (1986) Determination and analysis of urea and guanidine hydrochloride denaturation curves. *Methods Enzymol. 131*, 266−280.
(62) Mohana-Borges, R., Lima Silva, J., and de Prat-Gay, G. (1999) Protein folding in the absence of chemical denaturants. Reversible pressure denaturation of the noncovalent complex formed by the association of two protein fragments. *J. Biol. Chem. 274*, 7732−7740.
(63) Wyatt, P. J. (1993) Light scattering and the absolute characterization of macromolecules. *Anal. Chim. Acta 272*, 1−40.
(64) Li, S., Xing, D., and Li, J. (2004) Dynamic light scattering application to study protein interactions in electrolyte solutions. *J. Biol. Phys. 30*, 313−324.
(65) Lebowitz, J., Lewis, M. S., and Schuck, P. (2002) Modern analytical ultracentrifugation in protein science: a tutorial review. *Protein Sci. 11*, 2067−2079.
(66) Arthur, K. K., Gabrielson, J. P., Kendrick, B. S., and Stoner, M. R. (2009) Detection of protein aggregates by sedimentation velocity analytical ultracentrifugation (SV-AUC): sources of variability and their relative importance. *J. Pharm. Sci. 98*, 3522−3539.

(67) Fontana, A., de Laureto, P. P., Spolaore, B., Frare, E., Picotti, P., and Zambonin, M. (2004) Probing protein structure by limited proteolysis. *Acta Biochim. Pol. 51*, 299−321.
(68) Singh, S. M., Molas, J. F., Kongari, N., Bandi, S., Armstrong, G. S., Winder, S. J., and Mallela, K. M. (2012) Thermodynamic stability, unfolding kinetics, and aggregation of the N-terminal actin-binding domains of utrophin and dystrophin. *Proteins 80*, 1377−1392.
(69) Latypov, R. F., Liu, D., Jacob, J., Harvey, T. S., Bondarenko, P. V., Kleemann, G. R., Brems, D. N., and Raibekas, A. A. (2009) Denaturant-dependent conformational changes in a beta-trefoil protein: global and residue-specific aspects of an equilibrium denaturation process. *Biochemistry 48*, 10934−10947.
(70) Woody, R. W. (1996) Circular dichroism and conformational analysis of biomolecules, in *Theory of Circular Dichroism of Proteins*, p 25, Plenum Press, New York.
(71) Harn, N, S, T., Perkins, M, Allan, C, Shire, S. J., and CR, M. (2010) Biophysical signature of monoclonal antibodies, in *Current Trends in Monoclonal Antibodies Development and Manufacturing* (Shire, S. J., Gombotz, W., Bechtold-Peters, K, and Andya, J, Eds.) pp 229−248, Springer, New York.
(72) Bhambhani, A., Kissmann, J. M., Joshi, S. B., Volkin, D. B., Kashi, R. S., and Middaugh, C. R. (2012) Formulation design and high-throughput excipient selection based on structural integrity and conformational stability of dilute and highly concentrated IgG1 monoclonal antibody solutions. *J. Pharm. Sci. 101*, 1120−1135.
(73) Shi, S., Liu, J., Joshi, S. B., Krasnoperov, V., Gill, P., Middaugh, C. R., and Volkin, D. B. (2012) Biophysical characterization and stabilization of the recombinant albumin fusion protein sEphB4-HSA. *J. Pharm. Sci. 101*, 1969−1984.
(74) Matsuura, J. E., and Manning, M. C. (1994) Heat-induced gel formation of β-lactoglobulin: a study on the secondary and tertiary structure as followed by circular dichroism spectroscopy. *J. Agric. Food Chem. 42*, 1650−1656.
(75) Brych, S. R., Gokarn, Y. R., Hultgen, H., Stevenson, R. J., Rajan, R., and Matsumura, M. (2010) Characterization of antibody aggregation: role of buried, unpaired cysteines in particle formation. *J. Pharm. Sci. 99*, 764−781.
(76) Oganesyan, V., Damschroder, M. M., Leach, W., Wu, H., and Dall'Acqua, W. F. (2008) Structural characterization of a mutated, ADCC-enhanced human Fc fragment. *Mol. Immunol. 45*, 1872−1882.
(77) Bai, Y., Sosnick, T. R., Mayne, L., and Englander, S. W. (1995) Protein folding intermediates: native-state hydrogen exchange. *Science 269*, 192−197.
(78) Radford, S. E., Buck, M., Topping, K. D., Dobson, C. M., and Evans, P. A. (1992) Hydrogen exchange in native and denatured states of hen egg-white lysozyme. *Proteins 14*, 237−248.
(79) Uversky, V. N. (2013) Under-folded proteins: conformational ensembles and their roles in protein folding, function, and pathogenesis. *Biopolymers 99*, 870−887.
(80) Brummitt, R. K., Nesta, D. P., Chang, L., Kroetsch, A. M., and Roberts, C. J. (2011) Nonnative aggregation of an IgG1 antibody in acidic conditions, part 2: nucleation and growth kinetics with competing growth mechanisms. *J. Pharm. Sci. 100*, 2104−2119.
(81) Latypov, R. F., Hogan, S., Lau, H., Gadgil, H., and Liu, D. (2012) Elucidation of acid-induced unfolding and aggregation of human immunoglobulin IgG1 and IgG2 Fc. *J. Biol. Chem. 287*, 1381−1396.
(82) Arosio, P., Rima, S., and Morbidelli, M. (2013) Aggregation mechanism of an IgG2 and two IgG1 monoclonal antibodies at low pH: from oligomers to larger aggregates. *Pharm. Res. 30*, 641−654.
(83) Kiese, S., Papppenberger, A., Friess, W., and Mahler, H. C. (2008) Shaken, not stirred: mechanical stress testing of an IgG1 antibody. *J. Pharm. Sci. 97*, 4347−4366.
(84) Maa, Y. F., and Hsu, C. C. (1997) Protein denaturation by combined effect of shear and air-liquid interface. *Biotechnol. Bioeng. 54*, 503−512.
(85) Kreilgaard, L., Jones, L. S., Randolph, T. W., Frokjaer, S., Flink, J. M., Manning, M. C., and Carpenter, J. F. (1998) Effect of Tween 20 on freeze-thawing- and agitation-induced aggregation of recombinant human factor XIII. *J. Pharm. Sci. 87*, 1597−1603.
(86) Barnard, J. G., Singh, S., Randolph, T. W., and Carpenter, J. F. (2011) Subvisible particle counting provides a sensitive method of detecting and quantifying aggregation of monoclonal antibody caused by freeze-thawing: insights into the roles of particles in the protein aggregation pathway. *J. Pharm. Sci. 100*, 492−503.
(87) Cordes, A. A., Carpenter, J. F., and Randolph, T. W. (2012) Accelerated stability studies of abatacept formulations: comparison of freeze-thawing- and agitation-induced stresses. *J. Pharm. Sci. 101*, 2307−2315.
(88) Strucksberg, K. H., Rosenkranz, T., and Fitter, J. (2007) Reversible and irreversible unfolding of multi-domain proteins. *Biochim. Biophys. Acta 1774*, 1591−1603.
(89) Wang, W., Singh, S., Zeng, D. L., King, K., and Nema, S. (2007) Antibody structure, instability, and formulation. *J. Pharm. Sci. 96*, 1−26.
(90) Honegger, A. (2008) Engineering antibodies for stability and efficient folding. *Handb. Exp. Pharmacol.*, 47−68.
(91) Hari, S. B., Lau, H., Razinkov, V. I., Chen, S., and Latypov, R. F. (2010) Acid-induced aggregation of human monoclonal IgG1 and IgG2: molecular mechanism and the effect of solution composition. *Biochemistry 49*, 9328−9338.
(92) Park, C., and Marqusee, S. (2004) Probing the high energy states in proteins by proteolysis. *J. Mol. Biol. 343*, 1467−1476.
(93) Fontana, A., Polverino de Laureto, P., De Filippis, V., Scaramella, E., and Zambonin, M. (1997) Probing the partly folded states of proteins by limited proteolysis. *Folding Des. 2*, R17−26.
(94) Crisman, R. L., and Randolph, T. W. (2009) Refolding of proteins from inclusion bodies is favored by a diminished hydrophobic effect at elevated pressures. *Biotechnol. Bioeng. 102*, 483−492.
(95) Liu, W., Cellmer, T., Keerl, D., Prausnitz, J. M., and Blanch, H. W. (2005) Interactions of lysozyme in guanidinium chloride solutions from static and dynamic light-scattering measurements. *Biotechnol. Bioeng. 90*, 482−490.
(96) Kendrick, B. S., Cleland, J. L., Lam, X., Nguyen, T., Randolph, T. W., Manning, M. C., and Carpenter, J. F. (1998) Aggregation of recombinant human interferon gamma: kinetics and structural transitions. *J. Pharm. Sci. 87*, 1069−1076.
(97) Apostol, M. I., Perry, K., and Surewicz, W. K. (2013) Crystal structure of a human prion protein fragment reveals a motif for oligomer formation. *J. Am. Chem. Soc. 135*, 10202−10205.
(98) Mason, B. D., Schoneich, C., and Kerwin, B. A. (2012) Effect of pH and light on aggregation and conformation of an IgG1 mAb. *Mol. Pharm. 9*, 774−790.
(99) Das, P., King, J. A., and Zhou, R. (2011) Aggregation of gamma-crystallins associated with human cataracts via domain swapping at the C-terminal beta-strands. *Proc. Natl. Acad. Sci. U.S.A. 108*, 10514−10519.
(100) Randolph, T. W., Seefeldt, M., and Carpenter, J. F. (2002) High hydrostatic pressure as a tool to study protein aggregation and amyloidosis. *Biochim. Biophys. Acta 1595*, 224−234.
(101) St. John, R. J., Carpenter, J. F., and Randolph, T. W. (1999) High pressure fosters protein refolding from aggregates at high concentrations. *Proc. Natl. Acad. Sci. U.S.A. 96*, 13029−13033.
(102) Narhi, L. O., Schmit, J., Bechtold-Peters, K., and Sharma, D. (2012) Classification of protein aggregates. *J. Pharm. Sci. 101*, 493−498.